ISSN: 2998-2707

Anatomy & Physiology: Open Access Journal

DOI: 10.33552/APOAJ.2026.02.000533

Iris Publishers

Review article



# Morphology, Topography, and Extraluminal Morphometry of the Middle Cerebral Artery (sylvian artery) by Vascular Injection and Dissection

**Racky Wade[1]*, Magaye Gaye[1], Ainina Ndiaye[1], Abdoulaye Ndiaye[1], Mamadou Diop[1] and Jean-Marc Ndiaga Ndoye[1]**

*[1]Laboratory of Anatomy and Organogenesis (LOAD), Faculty of Medicine, Pharmacy and Odontology, Cheikh Anta Diop University (UCAD), Dakar, Senegal*

***Corresponding author:** Racky Wade, Laboratory of Anatomy and Organogenesis (LOAD), Faculty of Medicine, Pharmacy and Odontology, Cheikh Anta Diop University (UCAD), Dakar, Senegal

**Received Date:** January 16, 2026

**Published Date:** February 23, 2026

## Introduction

The middle cerebral artery (MCA), also known as the sylvian artery, is the largest terminal branch of the internal carotid artery and represents the principal hemodynamic axis of lateral hemispheric vascularization. It supplies a wide portion of the cerebral convexity, including the primary motor and sensory cortices, auditory areas, language-related regions, as well as the insular territory, a deep cortical structure with complex integrative functions [1,2]. The insula plays a key role in interoceptive perception, multimodal sensory integration, emotional regulation, autonomic nervous system control, and several cognitive and behavioral dimensions, as demonstrated by contemporary neuroanatomical and neurofunctional studies [3,4]. Its vascular supply is provided almost exclusively by the deep segments of the MCA, particularly the insular segment (M2) and its perforating branches, conferring to this artery a decisive role in the clinical expression of sylvian lesions [1,5]. This extensive functional distribution explains why involvement of the MCA may result in complex neurological, neuropsychological, or neuropsychiatric syndromes, combining motor and sensory deficits, language disorders, cognitive impairment, and emotional disturbances [3,6].

In clinical practice, the MCA is frequently involved in ischemic and hemorrhagic cerebrovascular events, while in neurosurgery and interventional neuroradiology it constitutes a central vascular axis for the treatment of aneurysms, vascular malformations, and deep lesions of the sylvian region [2,7,8]. From an anatomical and microsurgical perspective, the MCA is classically subdivided into four successive segments: the M1 or sphenoidal segment, with a basal and transverse course; the M2 or insular segment, located deep within the lateral cerebral fossa; the M3 or opercular segment, situated between the two lips of the lateral sulcus; and the M4 or cortical segment, corresponding to the terminal branches on the surface of the cerebral convexity [1,7]. This segmentation has major descriptive and topographical value, allowing precise localization of arterial division sites (bifurcations or trifurcations), identification of superficial cortical branches, and, most importantly, recognition of deep perforating arteries-particularly the lenticulostriate arteries—whose integrity directly determines postoperative functional outcome [2,5,9]. Anatomical investigations, particularly those based on microsurgical dissection with vascular injection, have demonstrated marked interindividual variability of the MCA.

This variability involves the number of arterial trunks, division patterns, length and caliber of the M1 segment, as well as the spatial organization of segments M2 to M4 and the distribution of cortical and perforating branches [7,10]. It partly accounts for the heterogeneity observed in clinical and radiological presentations of sylvian territory lesions and for the technical complexity encountered during surgical or endovascular procedures. The lateral cerebral fossa represents a key operative space for transsylvian approaches.

Its three-dimensional morphology, shaped by the organization of deep subarachnoid compartments, directly determines the course of the MCA and its secondary trunks. A detailed understanding of the relationships between MCA segments, the compartments of the lateral fossa, insular reliefs, and opercular structures is essential to reduce the risk of perioperative ischemic complications and to improve interpretation of neuroimaging data [7,9,11]. Anatomical studies have further shown that the distribution of cortical territories of the major cerebral arteries, particularly the MCA, exhibits significant interindividual variability, both morphologically and topographically. Consequently, standardized anatomical descriptions of the middle cerebral artery do not always reflect the individual vascular anatomy encountered in clinical or surgical settings.

This observation justifies the need for detailed morphological studies combining fine topographical analysis with quantitative morphometric data, in order to improve correlations between anatomical findings, imaging data, and clinical manifestations [10,12]. In African populations, specific anatomical and morphometric data on the MCA remain limited. Imaging-based studies using magnetic resonance imaging or angiography provide valuable but indirect information and are subject to technical constraints, particularly regarding assessment of true vessel caliber and interindividual variability of vascular territories [13,8]. Previous magnetic resonance imaging studies have highlighted morphological and morphometric particularities of the MCA and the lateral fossa of brain, including the possibility of an arterial course along the central sulcus of the insula, as well as specific anatomo-functional correlations [13-15]. These radiological observations raise the question of their true anatomical substrate and call for direct validation through vascular injection and dissection. The primary objective of this study was to describe, in autopsied adult brains, the morphology, topography, and morphometry of the middle cerebral artery. More specifically, the study aimed to analyze MCA division patterns and the number of arterial trunks at each segment, to characterize the segmental course of the artery within the different compartments of the lateral cerebral fossa, including the central sulcus of the insula and to measure extraluminal diameters at the origins of segments M1 to M4, and to assess potential associations with cerebral hemisphere, sex, and age.

## Methodology

### Study design and period

This was an observational, descriptive, topographical, and morphometric anatomical study with an analytical purpose, conducted using a prospective and continuous day-to-day recruitment over a three-month period (June to August 2025), during medicolegal autopsies. The study design complied with methodological recommendations applicable to human anatomical research, particularly the Anatomical Quality Assurance (AQUA) guidelines for anatomical reporting and the STROBE statement for observational studies [16,17].

### Anatomical specimens

The study was carried out on brains obtained from adult autopsied subjects and preserved under standardized conditions. Inclusion criteria were: age ≥ 17 years; a post-mortem interval of less than 48 hours; and absence of macroscopic signs of decomposition. Exclusion criteria included: macroscopic cranioencephalic lesions and a known history of neurological or neurosurgical disease. A total of 20 subjects, corresponding to 40 cerebral hemispheres, were included.

### Materials

The materials used included: transparent epoxy resin; isopropyl alcohol (propan-2-ol) 99–99.8%; red powdered pigment; graduated mixing cups and a manual stirrer; 5-mL syringes; flexible 18-gauge catheters; a dissection box and surgical instruments; fine dissection instruments (forceps, scissors, needles); a digital caliper with micrometer; physiological saline solution; storage containers; personal protective equipment (FFP2 masks, safety goggles, surgical gowns, gloves); a high-definition smartphone for photographic documentation; and an electric saw with craniotomy equipment.

## Method

### Craniotomy and brain extraction

The autopsied subject was placed in the supine position. A coronal scalp incision was made from one ear to the other, followed by blunt separation of the soft tissues. The scalp was reflected anteriorly and posteriorly to expose the calvaria. A horizontal circular craniotomy was then performed using an electric saw, allowing careful elevation of the cranial vault and exposure of the dura mater. The dura mater was subsequently incised cautiously along the interhemispheric fissure, with particular care taken to preserve the underlying cerebral structures (Figure 1). The extraction began with gentle retraction of the frontal lobes.

The optic nerves were sectioned as distally as possible using fine scissors, while minimizing any trauma to the internal carotid arteries, which were subsequently freed at the level of the anterior clinoid processes. The tentorium cerebelli was then incised along its greater circumference, from anterior to posterior, allowing access to the remaining cranial nerves, which were sequentially detached from the skull base. The brainstem was sectioned at the level of the bulb medullary junction, allowing complete release of the brain (Figure 1). The brain, extracted en bloc, was thoroughly rinsed with water and then allowed to rest for five minutes in an inferior surface–down position to facilitate drainage of residual blood prior to vascular injection.

### Catheterization of the middle cerebral artery

The internal carotid arteries were identified, and a flexible 18-gauge catheter (green) was introduced into each middle cerebral artery. The catheter was advanced to approximately 1 cm distal to the origin of the M1 segment and secured in position using a non-toothed clamp to prevent retrograde leakage of resin during injection.

## Preparation and Injection of the Resin Mixture

The epoxy resin (component A) was fluidified by the gradual addition of analytical-grade isopropyl alcohol (approximately 3% of the total volume) and subsequently colored by adding red pow-

dered pigment (1–2% of the resin weight). The mixture was slowly homogenized to obtain a fluid, uniform, and bubble-free solution and was used immediately after preparation (Figure 2&3). The injection was performed manually using a 5-mL syringe, applying gentle, continuous, and progressive pressure under direct visual monitoring of the filling of the middle cerebral artery arterial network, while carefully avoiding any overdistension.

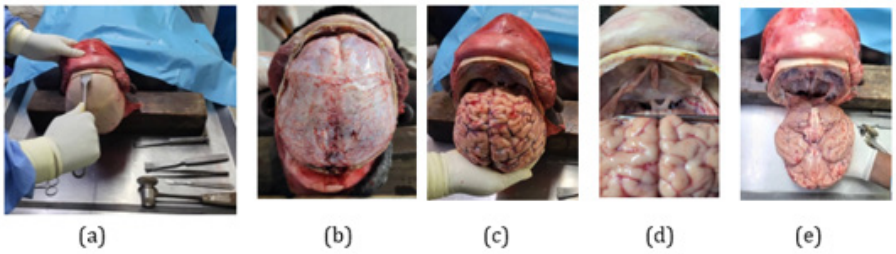


**Figure 1:** Circular craniotomy (a), exposure of the dura mater (b), retraction of the frontal lobes (c), section of the optic nerves (d), and extraction of the brain (e).

**Figure 2:** Transparent epoxy resin + isopropyl alcohol + red powdered pigment forming a homogenized mixture.

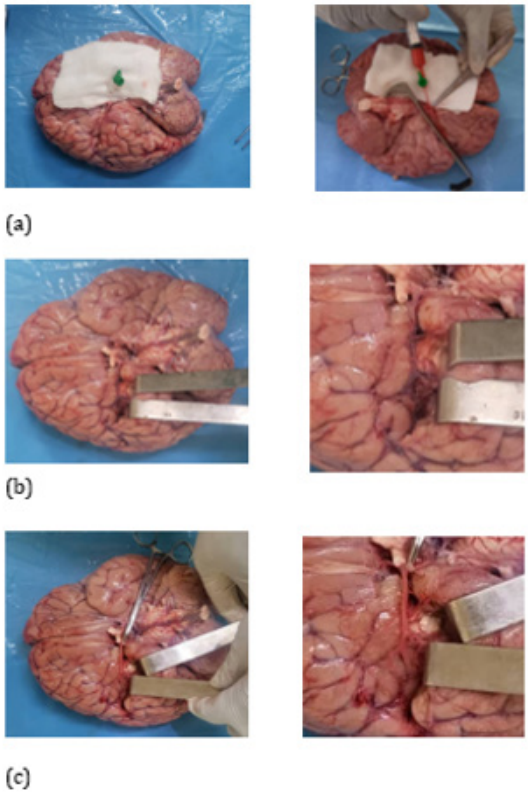


**Figure 3:** Catheterization and vascular injection (a), M1 segment before injection (b), and M1 segment after injection (c).

## Dissection of the Lateral Fissure of the Brain and the Middle Cerebral Artery

The brain was positioned in a stable manner, with its inferior surface facing downward and observed from a superior view. This orientation allowed passive opening of the lateral fissure without excessive traction on the frontal and temporal lobes. Dissection began with macroscopic exposure of the lateral fissure of the brain. The frontal and temporal lobes were gently separated to clearly visualize the sphenoidal margin of the arachnoid membrane. Opening of the arachnoid plane constituted the first step of fine dissection. The arachnoid was incised longitudinally along the lateral fissure using fine dissection scissors. Arachnoid trabeculae were progressively divided by blunt dissection, advancing the tip of a fine, non-toothed forceps between the arachnoid layers, without applying direct traction to the vessels.

The ascending and descending branches of the middle cerebral artery, rendered visible by the injection of colored resin, were gradually individualized. Their exposure was achieved by gentle separation of the inner surface of the arachnoid membrane. After complete opening of the lateral fissure by progressive separation of its two lips, the topographical arrangement of the arterial network was analyzed *in situ*. At this stage, a detailed cartography of the middle cerebral artery was established and documented by standardized photography and schematic drawings prior to any detachment of the pia mater, in order to preserve the initial anatomical configuration. Vascular dissection was subsequently continued by progressive detachment of the pia mater surrounding the arterial trunks.

This step allowed complete exposure of the middle cerebral artery from its origin to its terminal branches, including segments M1, M2, M3, and M4, together with their division branches. Dissection progressed along an anteroposterior axis and from medial to lateral, ensuring accurate identification of anatomical relationships and minimizing secondary displacement of vascular structures. All manipulations were performed under constant illumination to ensure optimal visualization of the structures studied (Figure 4). This dissection methodology allowed a reliable combined morphological, topographical, and morphometric analysis, while preserving the true anatomical configuration of the arterial network of the middle cerebral artery.

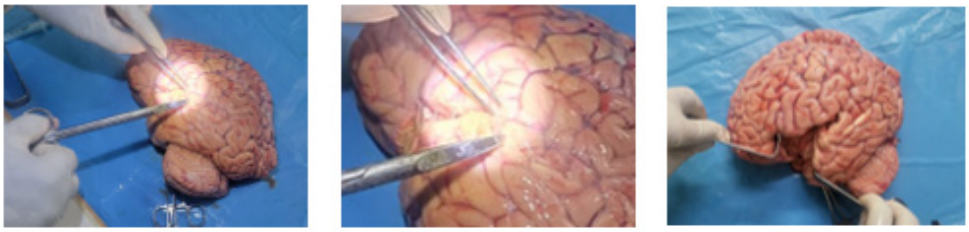

**Figure 4:** Dissection of the arachnoid membrane along the lateral fissure followed by opening of the lateral fissure of the brain.

## Morphological, Topographical, and Morphometric Analysis

### Morphological and topographical analysis

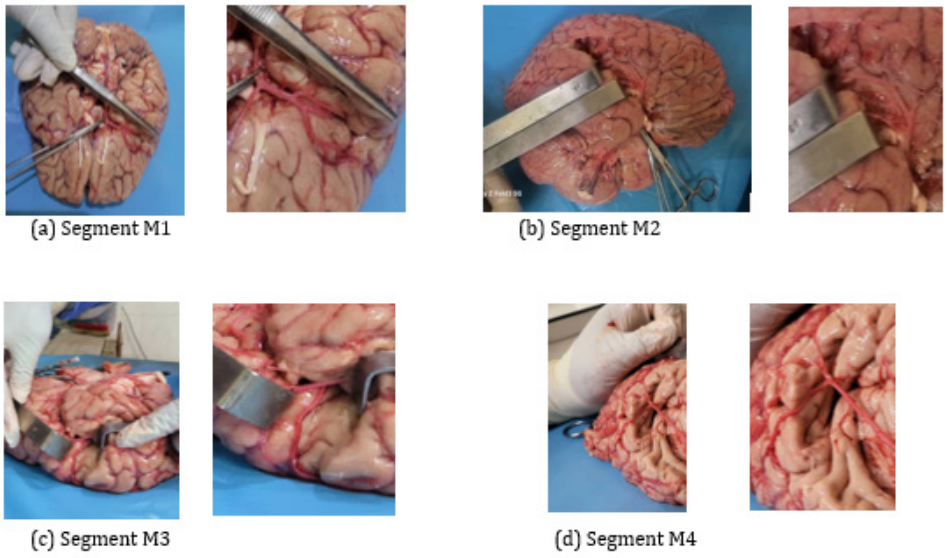


**Figure 5:** Segments of MCA.

Morphological analysis was based on a systematic and standardized identification of the middle cerebral artery from its origin to its termination (Figure 5).

For each cerebral hemisphere, the following parameters were determined:

- The number of arterial trunks at the origin of the middle cerebral artery (MCA) and at each of its segments (M1 to M4);
- The course of each segment and its possible secondary trunks through the anatomical compartments of the lateral fissure of the brain.

Within its deep subarachnoid space, the lateral fissure of the brain was subdivided into four constant compartments. The lateral opening corresponding to the lateral fissure itself constituted a fifth compartment. In accordance with our previous work, the central sulcus of the insula was considered an additional distinct anatomical area [13]. The main trunk was defined as the trunk exhibiting the largest extraluminal diameter. The remaining trunks were classified as secondary trunks in decreasing order of caliber.

### Morphometric analysis

Morphometric analysis consisted of measuring the extraluminal diameter of the middle cerebral artery at the origins of segments M1 (sphenoidal), M2 (insular or sylvian), M3 (opercular), and M4 (cortical). Segmental origins were identified using constant and reproducible anatomical landmarks of the lateral fissure of the brain, namely the termination of the internal carotid artery for M1, the apex of the insula (limen insulae) for M2, the lateral fissure and its lips for M3, and the superficial cerebral cortex for M4 [18].

Extraluminal diameter measurements were performed using a previously calibrated digital caliper. Each vessel was measured *in situ*, without vascular sectioning, perpendicular to its longitudinal axis, with light contact on the adventitia and without compression. Each measurement was performed twice, with complete repositioning of the instrument, and the mean value was recorded. Measurements were carried out successively on the right and left middle cerebral arteries, following a constant order (M1, M2, M3, M4), ensuring intra-observer reproducibility (Figure 5).

## Data Analysis

Data were analyzed using SPSS software, version 25.0. Qualitative variables were described using frequencies and percentages. Normality of quantitative data distributions was assessed using the Shapiro–Wilk test. Intersegmental comparisons were performed using the Wilcoxon signed-rank test for paired data. Correlations were analyzed using Spearman's rank correlation coefficient. Comparisons according to sex were conducted using the Mann–Whitney U test. Multiple linear regression analysis, adjusted for the number of arterial trunks, was used to identify determinants of intersegmental diameter variations. The level of statistical significance was set at 5%.

## Ethical Considerations

The study was conducted following institutional authorization, in accordance with ethical regulations governing medicolegal autopsies and the use of human anatomical material, without any irreversible alteration not justified by the scientific objectives.

## Results

### General characteristics of the studied subjects

Twenty (20) subjects were included, representing forty (40) cerebral hemispheres. Age ranged from 17 to 60 years, with a mean age of 40.7 ± 12.8 years. The study population was predominantly male (15/20; 75%). Marital status was mainly single (9/20; 45%). Tobacco and/or alcohol consumption was reported in 3 subjects (15%). Medical, gynecological–obstetric (in female subjects), and psychiatric histories were reported in 4 subjects (20%), 5 subjects (25%), and 2 subjects (10%), respectively. The post-mortem interval was less than 24 hours in 17 subjects (85%) and between 24 and 48 hours in 3 subjects (15%) (Table 1).

**Table 1:** General characteristics of the study subjects.

| General characteristics | Values |
|---|---|
| Mean age ± standard deviation (years) | 40.7 ± 12.8 |
| Minimum age (years) | 17 |
| Maximum age (years) | 60 |
| **Age groups, n (%)** | |
| < 20 years | 1 (5) |
| 20–29 years | 4 (20) |
| 30–39 years | 2 (10) |
| 40–49 years | 7 (35) |
| 50–59 years | 5 (25) |
| ≥ 60 years | 1 (5) |
| Sex, n (%) | |
| Male | 15 (75) |

| | |
|---|---|
| Female | 5 (25) |
| **Marital status, n (%)** | |
| Single | 9 (45) |
| Married | 7 (35) |
| Divorced | 1 (5) |
| Not reported | 3 (15) |
| **Lifestyle habits, n (%)** | |
| None | 17 (85) |
| Tobacco use | 2 (10) |
| Tobacco + alcohol use | 1 (5) |
| **Medical history, n (%)** | |
| None | 16 (80) |
| Hypertension + diabetes | 1 (5) |
| Other | 3 (15) |
| **Gynecological–obstetric history (women), n (%)** | |
| Yes | 5 (25) |
| No | 15 (75) |
| **Psychiatric history, n (%)** | |
| Yes | 2 (10) |
| No | 18 (90) |
| **Current treatment, n (%)** | |
| Yes | 3 (15) |
| No | 17 (85) |
| **Post-mortem interval, n (%)** | |
| < 24 hours | 17 (85) |
| 24–48 hours | |

## Morphology: number of arterial trunks and division patterns

### Segmental analysis

The distribution of the number of arterial trunks visualized for each segment of the middle cerebral artery (MCA), in both cerebral hemispheres, is presented in Table 2. In both hemispheres, a single trunk was constant at the origin of the MCA and at the level of the M1 segment (20/20; 100%). In the right cerebral hemisphere (RCH), the M2 segment exhibited a single trunk in 75% of cases, two trunks in 20%, and three trunks in 5%. In the M3 and M4 segments, a single trunk was observed in 75% of cases, with distributions including duplications (15%), triplications (5%), and one case with four trunks (5%). In the left cerebral hemisphere (LCH), the M2, M3, and M4 segments showed an identical distribution: a single trunk in 65% of cases, two trunks in 25%, and three trunks in 10% (Table 2).

**Table 2:** Distribution of the number of arterial trunks visualized in each segment of the middle cerebral artery in both cerebral hemispheres.

| MCA Segments | RCH<br>N (%) | LCH<br>N (%) |
|---|---|---|
| Origin | | |
| 1 | 20 (100) | 20 (100) |
| 2 | 0 (0) | 0 (0) |
| 3 | 0 (0) | 0 (0) |
| 4 | 0 (0) | 0 (0) |
| M1 | | |
| 1 | 20 (100) | 20 (100) |

| | | |
|---|---|---|
| 2 | 0 (0) | 0 (0) |
| 3 | 0 (0) | 0 (0) |
| 4 | 0 (0) | 0 (0) |
| M2 | | |
| 1 | 15 (75) | 13 (65) |
| 2 | 4 (20) | 5 (25) |
| 3 | 1 (5) | 2 (10) |
| 4 | 0 (0) | 0 (0) |
| M3 | | |
| 1 | 15 (75) | 13 (65) |
| 2 | 3 (15) | 5 (25) |
| 3 | 1 (5) | 2 (10) |
| 4 | 1 (5) | 0 (0) |
| M4 | | |
| 1 | 15 (75) | 13 (65) |
| 2 | 3 (15) | 5 (25) |
| 3 | 1 (5) | 2 (10) |
| 4 | 1 (5) | 0 (0) |

**Anatomical division patterns of the middle cerebral artery**

Division of a single arterial segment into two trunks was defined as a bifurcation, whereas division into three trunks corresponded to a trifurcation. The trunks arising from these divisions displayed a divergent orientation, associated with focal enlargement of the arterial caliber at the division point. In the right cerebral hemisphere, a single trunk was observed in 75% of cases (15/20), a bifurcation in 20% (4/20), and a trifurcation in 5% (1/20). Overall, arterial division occurred preferentially distal to the M1 segment. In the left cerebral hemisphere, a single trunk was observed in 65% of cases (13/20), a bifurcation in 25% (5/20), and a trifurcation in 10% (2/20). A rare anatomical variation was observed in one case, characterized by an initial bifurcation of the M1 segment, followed by a secondary bifurcation of each resulting M2 trunk, leading to a quadrifid terminal distribution with four M3 trunks, each continuing as a cortical M4 branch. The collateral perforating branches observed were not included in the analysis of terminal division patterns (Figures 6-10).

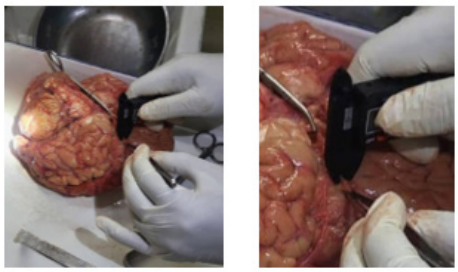

**Figure 6:** Measurement of the extraluminal diameter using a digital caliper.

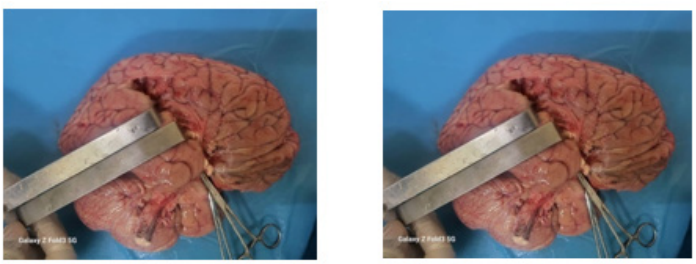

**Figure 7:** (a) In four cases, a single trunk persisted distal to the M1 segment in the right hemisphere.

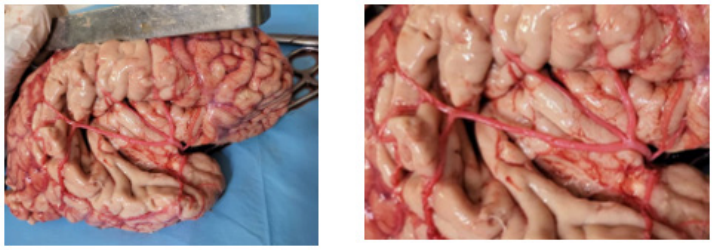

**Figure 7:** (b) A trifurcation distal to the M1 segment was observed in one right hemispheric case.

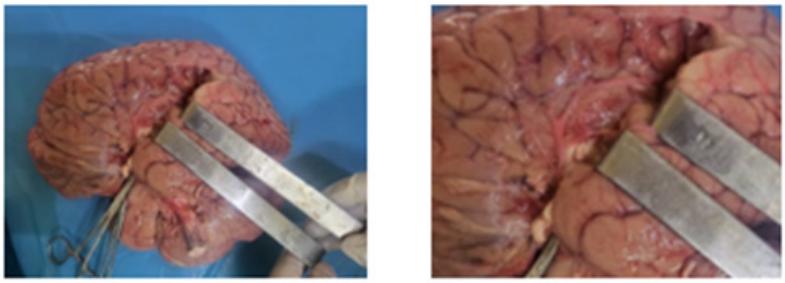

**Figure 8:** A single-trunk configuration of the middle cerebral artery was observed in the left cerebral hemisphere.

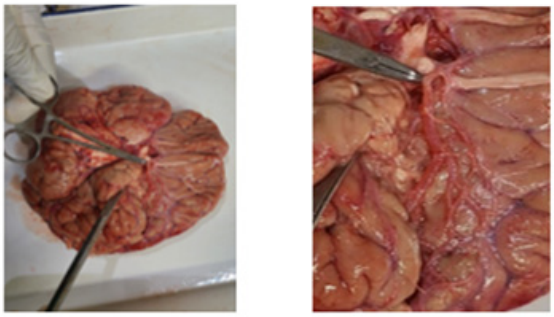

**Figure 9:** Bifurcation patterns was observed in the left cerebral hemisphere.

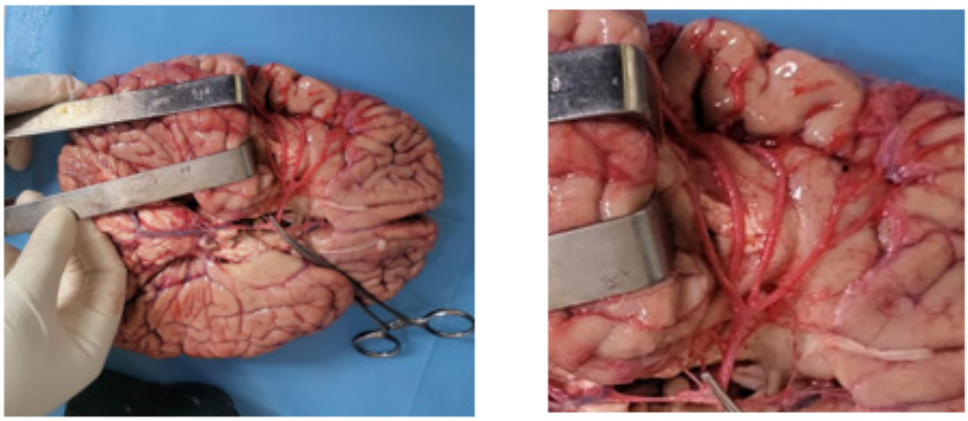

**Figure 10:** Variation with a quadrifid terminal division pattern. The collateral perforating branches observed were not included in the analysis of terminal division patterns.

## Topography: course of the middle cerebral artery within the compartments of the lateral fissure of the brain

### Right cerebral hemisphere

In the Right Cerebral Hemisphere (RCH), the course of the Middle Cerebral Artery (MCA) was analyzed for the Main Trunk (MT) and the Secondary Trunks (ST), segment by segment (M1 to M4), within the compartments of the lateral fissure of the brain. The percentages reported for each compartment are not mutually exclusive, as a given segment may successively traverse several compartments along its course. For the Main Trunk (MT), the M1 segment was constantly located within the sphenoidal compartment (20/20; 100%). At the level of the M2 segment, the course most frequently involved the inferior corridor compartments (C4: 45%; C3: 40%). The superior corridor compartments (C1 and C2) were each observed in 35% of cases. A course along the central sulcus of the insula (CSI) was identified in 25% of subjects (5/20). The M3 segment consistently traversed compartment C5 (20/20; 100%). The M4 segment was constantly located at the cortical level (20/20; 100%).

Regarding Secondary Trunk 1 (ST1), identified distal to a bifurcation or trifurcation, the M2 segment most commonly followed the superior corridor (C1: 15%; C2: 10%). Less frequent courses were observed within the inferior corridor (C3 or C4: 5% each), along the CSI (5%), and more rarely within the width of the lateral fissure itself (C5: 5%). The M3 segment most often traversed compartment C5 (25%). The M4 segment projected cortically onto the frontoparietal operculum (25%). Secondary Trunk 2 (ST2) was observed only in the context of a trifurcation (one case in the RCH). In this case, the M2 segment followed a course along the CSI; the M3 segment traversed compartment C5 (10%), and the M4 segment projected onto the cortical surface (10%). Secondary Trunk 3 (ST3) was identified in the quadrifid variation described above, corresponding to the fourth distal branch distinguishable from the M3 and M4 segments. In this case, the M3 segment traversed compartment C5 (5%), and the M4 segment extended to the cortical surface (5%) (Table 3).

**Table 3:** Description of the MCA course profile within the compartments of the lateral fossa of the brain in the right cerebral hemisphere.

| Segments | sphenoidal C<br>N (%) | C1<br>N (%) | C2<br>N (%) | C3<br>N (%) | C4<br>N (%) | SCI<br>N (%) | C5<br>N (%) | Cortex<br>N (%) |
|---|---|---|---|---|---|---|---|---|
| M1 | | | | | | | | |
| TP | 20 (100) | 0 (0) | 0 (0) | 0 (0) | 0 (0) | 0 (0) | 0 (0) | 0 (0) |
| TS1 | 0 (0) | 0 (0) | 0 (0) | 0 (0) | 0 (0) | 0 (0) | 0 (0) | 0 (0) |
| TS2 | 0 (0) | 0 (0) | 0 (0) | 0 (0) | 0 (0) | 0 (0) | 0 (0) | 0 (0) |
| TS3 | 0 (0) | 0 (0) | 0 (0) | 0 (0) | 0 (0) | 0 (0) | 0 (0) | 0 (0) |
| M2 | | | | | | | | |
| TP | 0 (0) | 7 (35) | 7 (35) | 8 (40) | 9 (45) | 5 (25) | 0 (0) | 0 (0) |
| TS1 | 0 (0) | 3 (15) | 2 (10) | 1 (5) | 1 (5) | 1 (5) | 1 (5) | 0 (0) |
| TS2 | 0 (0) | 0 (0) | 0 (0) | 0 (0) | 0 (0) | 1 (5) | 0 (0) | 0 (0) |
| TS3 | 0 (0) | 0 (0) | 0 (0) | 0 (0) | 0 (0) | 0 (0) | 0 (0) | 0 (0) |
| M3 | | | | | | | | |
| TP | 0 (0) | 0 (0) | 0 (0) | 0 (0) | 0 (0) | 0 (0) | 20 (100) | 0 (0) |
| TS1 | 0 (0) | 0 (0) | 0 (0) | 0 (0) | 0 (0) | 1 (5) | 5 (25) | 0 (0) |
| TS2 | 0 (0) | 0 (0) | 0 (0) | 0 (0) | 0 (0) | 1 (5) | 2 (10) | 0 (0) |
| TS3 | 0 (0) | 0 (0) | 0 (0) | 0 (0) | 0 (0) | 0 (0) | 1 (5) | 0 (0) |
| M4 | | | | | | | | |
| TP | 0 (0) | 0 (0) | 0 (0) | 0 (0) | 0 (0) | 0 (0) | 0 (0) | 20 (100) |
| TS1 | 0 (0) | 0 (0) | 0 (0) | 0 (0) | 0 (0) | 0 (0) | 0 (0) | 5 (25) |
| TS2 | 0 (0) | 0 (0) | 0 (0) | 0 (0) | 0 (0) | 0 (0) | 0 (0) | 2 (10) |
| TS3 | 0 (0) | 0 (0) | 0 (0) | 0 (0) | 0 (0) | 0 (0) | 0 (0) | 1 (5) |

### Distribution of the MCA course within the compartments of the lateral fossa of the brain in the left cerebral hemisphere

In the left cerebral hemisphere (LCH), the course of the middle cerebral artery (MCA) was analyzed for the main trunk (MT) and the secondary trunks (ST), segment by segment (M1 to M4), within the compartments of the lateral fissure of the brain. The percentages reported for each compartment are not mutually exclusive, as a given segment may successively traverse several compartments along its course. In all subjects, the M1 segment of the main trunk (MT) was located within the sphenoidal compartment (20/20; 100%). At the level of the M2 segment, the course preferentially involved the inferior corridor (C4: 45%; C3: 40%) and could also follow the superior corridor (C1: 35%; C2: 35%), as well as the central sulcus of the insula (CSI) (25%). A course within compartment

C5 was observed in one case (5%). The M3 segment traversed compartment C5 in all subjects (20/20; 100%), and the M4 segment was consistently located at the cortical level (20/20; 100%).

For secondary trunk 1 (ST1), present in cases of bifurcation or trifurcation, the M2 segment mainly followed compartment C1 (15%) and compartment C2 (10%), with a course along the CSI observed in 10% of cases and a course within compartment C4 in 5% of cases. The M3 segment traversed compartment C5 in 35% of cases, and the M4 segment projected onto the cortical surface in 35% of cases. For secondary trunk 2 (ST2), observed in cases of trifurcation, the M2 segment was identified within compartment C1 (5%), compartment C2 (5%), or along the CSI (5%). The M3 segment traversed compartment C5 in 10% of cases, and the M4 segment projected onto the cortical surface in 10% of cases (Table 4).

**Table 4:** Description of the MCA course profile within the compartments of the lateral fossa of the brain in the left cerebral hemisphere.

| Segments | sphenoidal C N (%) | C1 N (%) | C2 N (%) | C3 N (%) | C4 N (%) | SCI N (%) | C5 N (%) | Cortex N (%) |
|---|---|---|---|---|---|---|---|---|
| M1 | | | | | | | | |
| TP | 20 (100) | 0 (0) | 0 (0) | 0 (0) | 0 (0) | 0 (0) | 0 (0) | 0 (0) |
| ST 1 | 0 (0) | 0 (0) | 0 (0) | 0 (0) | 0 (0) | 0 (0) | 0 (0) | 0 (0) |
| ST 2 | 0 (0) | 0 (0) | 0 (0) | 0 (0) | 0 (0) | 0 (0) | 0 (0) | 0 (0) |
| ST 3 | 0 (0) | 0 (0) | 0 (0) | 0 (0) | 0 (0) | 0 (0) | 0 (0) | 0 (0) |
| M2 | | | | | | | | |
| MT | 0 (0) | 7 (35) | 7 (35) | 8 (40) | 9 (45) | 5 (25) | 1 (5) | 0 (0) |
| ST 1 | 0 (0) | 3 (15) | 2 (10) | 0 (0) | 1 (5) | 2 (10) | 1 (5) | 0 (0) |
| ST 2 | 0 (0) | 1 (5) | 1 (5) | 0 (0) | 0 (0) | 1 (5) | 0 (0) | 0 (0) |
| ST 3 | 0 (0) | 0 (0) | 0 (0) | 0 (0) | 0 (0) | 0 (0) | 0 (0) | 0 (0) |
| M3 | | | | | | | | |
| MT | 0 (0) | 0 (0) | 0 (0) | 0 (0) | 0 (0) | 0 (0) | 20 (100) | 0 (0) |
| ST 1 | 0 (0) | 0 (0) | 0 (0) | 0 (0) | 0 (0) | 0 (0) | 7 (35) | 0 (0) |
| ST 2 | 0 (0) | 0 (0) | 0 (0) | 0 (0) | 0 (0) | 0 (0) | 2 (10) | 0 (0) |
| ST 3 | 0 (0) | 0 (0) | 0 (0) | 0 (0) | 0 (0) | 0 (0) | 0 (0) | 0 (0) |
| M4 | | | | | | | | |
| MT | 0 (0) | 0 (0) | 0 (0) | 0 (0) | 0 (0) | 0 (0) | 0 (0) | 20 (100) |
| ST 1 | 0 (0) | 0 (0) | 0 (0) | 0 (0) | 0 (0) | 0 (0) | 0 (0) | 7 (35) |
| ST 2 | 0 (0) | 0 (0) | 0 (0) | 0 (0) | 0 (0) | 0 (0) | 0 (0) | 2 (10) |
| ST 3 | 0 (0) | 0 (0) | 0 (0) | 0 (0) | 0 (0) | 0 (0) | 0 (0) | 0 (0) |

**Modal morphological and topographical profile of the MCA**

The modal morphological profile corresponded to a subject aged 40–49 years presenting a single trunk at the origin and throughout segments M1 to M4 in both cerebral hemispheres. The modal course of the main trunk followed the sphenoidal compartment for M1, then the inferior corridor (C3–C4) for M2, the width of the lateral fissure (C5) for M3, and the cortical surface for M4.

## MCA morphometry

**Table 5:** Distribution of extraluminal diameters (mm) of the main trunk and secondary trunks of the MCA (right vs left cerebral hemispheres).

| Diameter | RCH | | | LCH | | |
|---|---|---|---|---|---|---|
| | Med (IIQ) | Min | Max | Med (IIQ) | Min | Max |
| MT | | | | | | |
| M1 | 2,2 (2,1 – 3,0) | 2,0 | 3,0 | 2,5 (2,2 – 3,0) | 2,0 | 3,0 |
| M2 | 2,0 (2,0 – 2,5) | 1,8 | 2,9 | 2,0 (2,0 – 2,2) | 1,5 | 3,0 |
| M3 | 1,7 (1,3 – 2,0) | 1,0 | 2,0 | 1,8 (1,5 – 2,0) | 1,0 | 2,0 |
| M4 | 1,0 (1,0 – 1,5) | 0,5 | 1,8 | 1,0 (1,0 – 1,3) | 0,9 | 1,8 |

| | | | | | | |
|---|---|---|---|---|---|---|
| ST 1 | | | | | | |
| M1 | 3,0 (2,6 – 3,0) | 2,1 | 3,0 | 3,0 (3,0 – 3,0) | 3,0 | 3,0 |
| M2 | 2,0 (1,9 – 2,1) | 1,5 | 2,5 | 2,0 (1,6 – 2,2) | 1,5 | 2,2 |
| M3 | 1,5 (1,2 – 1,6) | 1,0 | 1,8 | 1,6 (1,4 – 1,8) | 1,4 | 1,8 |
| M4 | 1,0 (0,9 – 1,1) | 0,8 | 1,5 | 1,0 (1,0 – 1,2) | 1,0 | 1,2 |
| ST 2 | | | | | | |
| M1 | 3,0 (3,0 – 3,0) | 3,0 | 3,0 | 3,0 (3,0 – 3,0) | 3,0 | 3,0 |
| M2 | 2,2 (1,8 – 2,2) | 1,8 | 2,2 | 1,8 (1,8 – 1,8) | 1,8 | 1,8 |
| M3 | 1,4 (1,2 – 1,4) | 1,2 | 1,5 | 1,6 (1,6 – 1,6) | 1,6 | 1,6 |
| M4 | 1,3 (1,0 – 1,3) | 1,0 | 1,5 | 1,0 (1,0 – 1,0) | 1,0 | 1,0 |
| ST 3 | | | | | | |
| M1 | 3,0 (2,1 – 3,0) | 2,0 | 3,1 | - | - | - |
| M2 | 2,3 (1,9 – 2,9) | 1,8 | 3,0 | - | - | - |
| M3 | 1,8 (1,5 – 1,9) | 1,5 | 2,0 | - | - | - |
| M4 | 1,3 (1,0 – 1,6) | 1,0 | 1,7 | - | - | - |

The distribution of extraluminal diameters of the main trunk (MT) and secondary trunks (ST) by segment (M1 to M4), in each cerebral hemisphere, is presented in Table 5. In both hemispheres, MT diameters progressively decreased from M1 to M4. At the M1 segment, in MCAs presenting secondary trunks in both hemispheres, the median diameter of the main trunk appeared greater than that observed in MCAs with a single trunk. The diameters of the secondary trunks (ST1 to ST3) are detailed in (Table 5).

**Intersegmental comparison of extraluminal diameters of the main trunk (Wilcoxon paired test)**

In both cerebral hemispheres, the diameter of the main trunk decreased significantly from one segment to the next from M1 to M4 (paired Wilcoxon test; $p < 0.001$) (Figures 11&12).

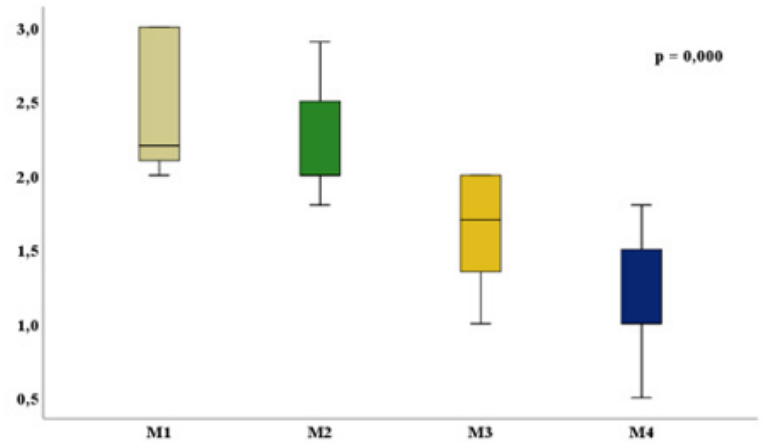


**Figure 11:** Comparative analysis of the main trunk diameter across segments in the right cerebral hemisphere.

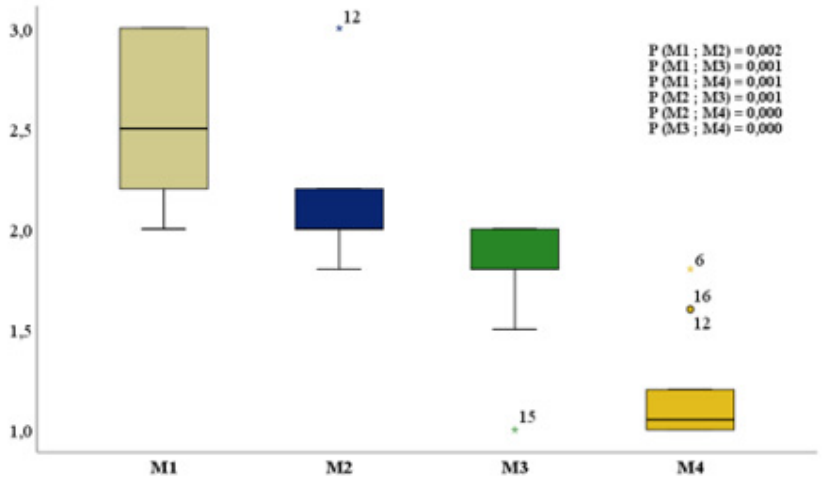


**Figure 12:** Comparative analysis of the main trunk diameter across segments in the left cerebral hemisphere.

**Intersegmental correlations of extraluminal diameters of the main trunk (Spearman's test)**

In the right cerebral hemisphere, a positive correlation was observed between the main trunk diameters of segments M1 and M2 (rho = 0.773; $p$ = 0.001), as well as between segments M3 and M4 (rho = 0.599; $p$ = 0.005). In the left cerebral hemisphere, a positive correlation was observed between segments M1 and M2 (rho = 0.613; $p$ = 0.020) (Tables 6&7).

Table 6: Intersegmental correlation analysis of the main trunk diameter in the right cerebral hemisphere.

| Segments | Parameters | M1 | M2 | M3 | M4 |
|---|---|---|---|---|---|
| M1 | Spearman's rho (ρ) | 1,000 | 0,773 | 0,242 | 0,169 |
| | p value | - | 0,001 | 0,303 | 0,477 |
| M2 | Spearman's rho (ρ) | 0,773 | 1,000 | 0,281 | 0,180 |
| | p value | 0,001 | - | 0,231 | 0,449 |
| M3 | Spearman's rho (ρ) | 0,242 | 0,281 | 1,000 | 0,599 |
| | p value | 0,303 | 0,231 | - | 0,005 |
| M4 | Spearman's rho (ρ) | 0,169 | 0,180 | 0,599 | 1,000 |
| | p value | 0,477 | 0,449 | 0,005 | - |

**Table 7:** Analyse de la correlation intersegmentaire du diamètre du tronc principal au niveau de l'HCG.

| Segments | Parameters | M1 | M2 | M3 | M4 |
|---|---|---|---|---|---|
| M1 | Spearman's rho (ρ) | 1,000 | 0,613 | 0,165 | -0,114 |
| | p value | - | 0,020 | 0,572 | 0,698 |
| M2 | Spearman's rho (ρ) | 0,613 | 1,000 | 0,366 | 0,221 |
| | p value | 0,020 | - | 0,148 | 0,393 |
| M3 | Spearman's rho (ρ) | 0,165 | 0,366 | 1,000 | 0,437 |
| | p value | 0,572 | 0,148 | - | 0,080 |
| M4 | Spearman's rho (ρ) | -0,114 | 0,221 | 0,437 | 1,000 |
| | p value | 0,698 | 0,393 | 0,080 | - |

**Comparison of extraluminal diameters of the main trunk according to sex (Mann–Whitney U test)**

In both cerebral hemispheres, main trunk diameters were comparable between males and females for each segment (Mann–Whitney U test; $p$ > 0.05) (Figures 13&14).

**Interhemispheric comparison of extraluminal diameters of the main trunk (paired Wilcoxon test)**

For each segment, the diameter of the main trunk did not differ significantly between the right and left cerebral hemispheres (paired Wilcoxon test; $p$ > 0.05) (Figure 15).

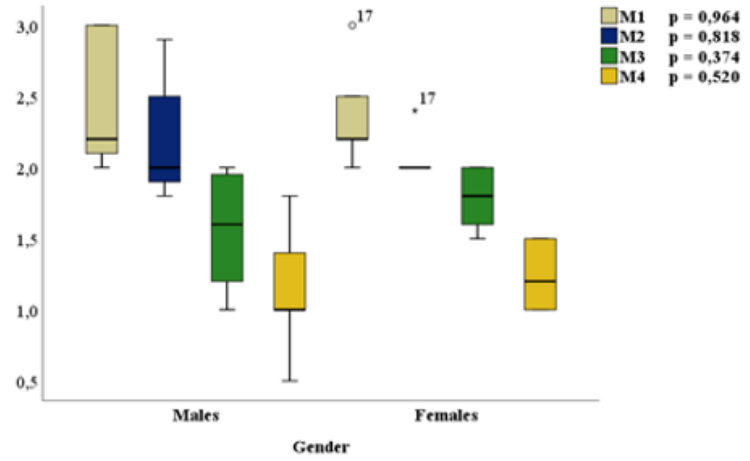


**Figure 13:** Comparative analysis of main trunk diameters across segments according to sex in the right cerebral hemisphere.

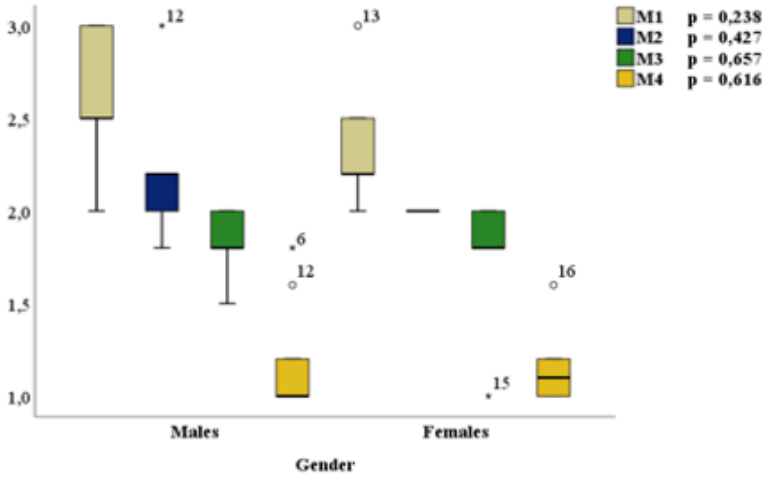


**Figure 14:** Comparative analysis of main trunk diameters across segments according to sex in the left cerebral hemisphere.

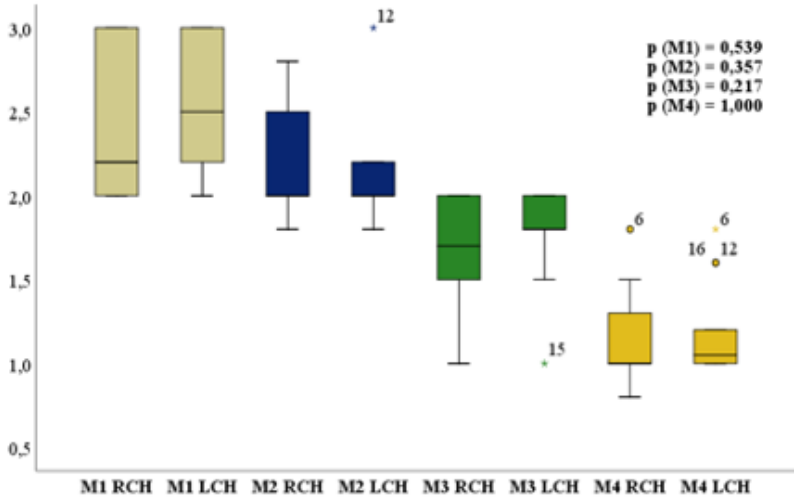


**Figure 15:** Comparative analysis of main trunk diameters across segments according to cerebral hemisphere.

**Correlation between age and main trunk diameters (Spearman's test)**

In the right cerebral hemisphere, age was positively correlated with main trunk diameters at segments M1 (rho = 0.660; *p*= 0.002) and M2 (rho = 0.512; *p* = 0.021). No significant correlation was observed in the left cerebral hemisphere ($p > 0.05$) (Table 8).

**Table 8:** Correlation analysis between main trunk diameters at each segment and age in both cerebral hemispheres.

| Hemisphere | Segments | Rho | p value |
|---|---|---|---|
| RCH | **M1** | **0,660** | **0,002** |
| | **M2** | **0,512** | **0,021** |
| | M3 | 0,352 | 0,128 |
| | M4 | 0,168 | 0,478 |
| LCH | M1 | 0,077 | 0,794 |
| | M2 | 0,388 | 0,111 |
| | M3 | 0,243 | 0,348 |
| | M4 | 0,224 | 0,388 |

**Determinants of main trunk diameter variations (multiple linear regression, right cerebral hemisphere)**

In the right cerebral hemisphere, the diameter of the main trunk at the M1 segment varied significantly according to the diameter of the main trunk at M2 (B = 0.969; 95% CI: 0.671–1.267; $p < 0.001$) and age (B=0.009; 95% CI:0.001–0.017; *p* =0.033). The diameter of the main trunk at the M2 segment varied significantly with that at M1 (B = 0.758; 95% CI: 0.525–0.992; $p < 0.001$). A covariance was also observed between segments M3 and M4 (M3–M4: *p* = 0.006; M4–M3: *p* = 0.007) (Table 9).

**Table 9:** Determinants of main trunk diameter variation by segment in the right cerebral hemisphere (multiple linear regression analysis).

| Segments | Determinants | Coefficient | 95% CI | p value |
|---|---|---|---|---|
| M1 | M2 | 0,969 | 0,671 – 1,267 | 0,001 |
| | Age | 0,009 | 0,001 – 0,017 | 0,033 |
| M2 | M1 | 0,758 | 0,525 – 0,992 | 0,001 |
| M3 | M4 | 0,656 | 0,215 – 1,098 | 0,006 |
| M4 | M3 | 0,524 | 0,167 – 0,882 | 0,007 |

## Discussion

### Synthesis of the main findings

This anatomical study, based on vascular injection and fine dissection of 40 adult cerebral hemispheres, provides an integrated description of the morphology, topography, and morphometry of the middle cerebral artery (MCA). The main findings highlight: (i) MCA division occurring preferentially distal to the M1 segment, with predominance of a single trunk, bifurcations being more frequent than trifurcations; (ii) marked topographical variability of the M2 segment within the compartments of the lateral fissure of the brain (LFB), including a substantial proportion of courses along the central sulcus of the insula (CSI); and (iii) a progressive decrease in extraluminal diameters of the main trunk from M1 to M4, associated with intersegmental correlations suggesting morphometric continuity along the main arterial axis.

### MCA morphology: segmental organization and division patterns

The constant presence of a single trunk at the level of the M1 segment observed in this series is consistent with classical anatomical descriptions of the MCA, in which M1 represents a relatively stable proximal segment, whereas morphological variability increases distally [1–5]. The segmentation of the MCA into sphenoidal (M1), insular (M2), opercular (M3), and cortical (M4) segments remains a relevant descriptive framework for anatomical and comparative analyses [1,7]. The division patterns observed from the M2 and M3 segments, including bifurcations, trifurcations, and more complex configurations, illustrate the diversity of terminal branching schemes previously reported in injection-based anatomical studies [2,5]. From a descriptive anatomy perspective, these findings confirm that simplified classifications of MCA division only partially reflect true anatomical diversity. The identification of rare configurations, such as the quadrifid distribution observed in one case, underscores the value of systematic cadaveric studies for documenting variants that are underrepresented in radiological or angiographic series.

### MCA topography: lateral fossa of brain compartments and the role of the CSI

One of the original contributions of this study lies in the detailed

topographical analysis of the MCA course within the compartments of the lateral fissure of the brain, in direct continuity with previous morphological descriptions of the sylvian valley [7,9]. The M2 segment of the main trunk preferentially followed the inferior corridor compartments (C3–C4), but could also traverse the superior corridor (C1–C2) or course along the central sulcus of the insula. The demonstration of an MCA course along the CSI in a substantial proportion of cases confirms that this insular landmark represents a relevant anatomical zone in the study of the sylvian region.

This observation is consistent with the three-dimensional complexity of the insula and the sylvian fissure described in microanatomical studies, where the relationships between M2 trunks, insular cortex, and opercular structures are highly variable [7]. It also illustrates how topographical variability of M2 trunks contributes to discrepancies between standardized anatomical schemes and actual individual anatomy. Beyond the sylvian region, vascular topographical variability is a major determinant of interindividual differences in cortical territories. The work of van der Zwan and colleagues demonstrated that the territories of major cerebral arteries, including the MCA, exhibit far greater variability than suggested by classical representations, reinforcing the relevance of detailed morphological and topographical approaches [10].

### Morphometry: hierarchical organization and segmental continuity

The progressive decrease in extraluminal diameters of the main trunk from M1 to M4 observed in this series corresponds to the expected hierarchical organization of the intracranial arterial tree. Injection-based anatomical studies have emphasized the relevance of the external (outer) diameter as a morphometric parameter in descriptive and microsurgical anatomy, particularly for comparative analysis of arterial segments [2]. The intersegmental correlations identified suggest morphometric continuity along the main trunk of the MCA, reflecting structural coherence of the arterial tree. The positive association observed between age and certain segmental diameters, limited to the right hemisphere, should be interpreted cautiously given the sample size, but remains compatible with published data describing age-related vascular remodeling, including changes in elastin content and arterial wall stiffness [11,13].

### Perforating branches: anatomical considerations

Although the primary objective of this study focused on the trunks and division segments of the MCA, the occasional observation of a collateral perforating branch supplying the insula highlights the anatomical importance of these deep branches. Perforators arising from proximal MCA segments supply critical deep structures such as the internal capsule and basal ganglia. Classical and contemporary anatomical studies have demonstrated wide variability in their number, caliber, and sites of origin, making their systematic anatomical characterization challenging but essential for understanding deep vascular architecture [18,16].

### Strengths, limitations, and anatomical perspectives

The main strength of this study lies in the combination of vascular injection with fine, compartment-based dissection, allowing an integrated morphological, topographical, and morphometric analysis of the MCA, in continuity with previous anatomical work on the sylvian valley [9]. Standardized segmental analysis and photographic documentation further enhance the descriptive value of the findings. Limitations primarily relate to sample size, the medicolegal context of the series, and the extraluminal nature of measurements obtained from post-mortem material, which are not directly comparable with in vivo luminal measurements from imaging studies. Future directions include expansion of the sample size, dedicated analysis of perforating branches, and incorporation of measurement reproducibility assessments, in accordance with anatomical quality guidelines (AQUA) and STROBE principles for observational studies [16,17].

## Conclusion

This anatomical study based on vascular injection and dissection provides an integrated morphological, topographical, and morphometric description of the middle cerebral artery in an adult autopsy series. It demonstrates variability in terminal division patterns, characterized by predominance of a single trunk, with less frequent bifurcations and trifurcations, as well as rare exceptional configurations. From a topographical perspective, the study reveals variability in the course of the M2 segment within the compartments of the lateral fissure of the brain, with a notable proportion of trajectories along the central sulcus of the insula, a feature of relevance for transsylvian approaches and preoperative anatomical assessment. From a quantitative standpoint, the study provides reference values for segmental extraluminal diameters (M1–M4) of the main trunk and secondary trunks, directly applicable to microsurgery, endovascular procedures, and imaging interpretation. Finally, these findings are consistent with and extend our previous MRI-based work, reinforcing the value of direct anatomical validation of sylvian variants. They provide a useful foundation for neurovascular anatomy teaching, surgical planning, and the development of multicenter anatomical studies, particularly in African settings [19-21].

## Conflict of Interest

The author declares that there are no conflicts of interest related to this study.

## Acknowledgements

The author would like to thank the entire staff of the Department of Anatomy and Pathological Cytology at Idrissa Pouye Hospital, Grand Yoff (Dakar, Senegal), for their support and for providing the opportunity to conduct this study.

## Use of Artificial Intelligence

A generative artificial intelligence tool (ChatGPT, OpenAI) was used in a limited manner for language editing, stylistic refinement, and improvement of manuscript clarity. No original data, scientific analyses, result interpretations, or methodological decisions were generated by this tool. The author takes full responsibility for the scientific content, data accuracy, interpretation of results, and the final version of the manuscript.

## References


1. Kamina P (2013) Neuroanatomie. Paris ; Maloine.
2. Rhoton AL (2002) The supratentorial arteries. Neurosurgery 51(4 Suppl): S53-S120.
3. Halama D, Merkel H, Werdehausen R, Gaber K, Schob S, et al. (2022) Reference values of cerebral artery diameters of the Anterior Circulation by Digital Subtraction Angiography : A Retrospective Study. Diagnostics (Basel) 12(10): 2471.
4. Fonck E, Feigl GG, Fasel J, Sage D, Unser M, et al. (2009) Effect of aging on elastin functionality in human cerebral arteries. Stroke 40(7): 2552-2556.
5. Gibo H, Carver CC, Rhoton AL, Lenkey C, Mitchell RJ (1981) Microsurgical anatomy of the middle cerebral artery. J Neurosurg 54(2): 151-169.
6. Marinković SV, Milisavljević MM, Kovacevic MS, Stevic ZD (1985) Perforating branches of the middle cerebral artery. Microanatomy and clinical significance of their intracerebral segments. Stroke 16(6): 1022-1029.
7. Umansky F, Juarez SM, Dujovny M, Ausman JI, Diaz FG, et al. (1984) Microsurgical anatomy of the proximal segments of the middle cerebral artery. J Neurosurg 61(3): 458-467.
8. Aydin IH, Takci E, Kadioglu HH, Kayaoglu CR, Barlas E (1996) Variations of the lenticulostriate arteries in the middle cerebral artery aneurysms. Acta Neurochir (Wien) 138(5): 555-559.
9. Tanriover N, Rhoton AL, Kawashima M, Ulm AJ, Yasuda A (2004) Microsurgical anatomy of the insula and the sylvian fissure. J Neurosurg 100(5): 891-922.
10. Elsharkawy A, Niemelä M, Lehečka M, Lehto H, Jahromi BR, et al. (2014) Focused opening of the sylvian fissure for microsurgical management of MCA aneurysms. Acta Neurochir (Wien) 156(1): 17-25.
11. Türe U, Yaşargil MG, Al-Mefty O, Yaşargil DC (2000) Arteries of the insula. J Neurosurg 92(4): 676–687.
12. van der Zwan A, Hillen B, Tulleken CA, Dujovny M, Dragovic L (1992) Variability of the territories of the major cerebral arteries. J Neurosurg 77(6) : 927-940.
13. Wade R, Plaisant O, Guédon A, Diop AD, Ndiaye A, et al. (2019) Morphology of the lateral fossa of the brain (sylvian valley) : anatomo-radiological aspects and surgical application. Surg Radiol Anat 41(6): 639-655.
14. Wade R, Ndiaye M, Gaye M, Ndiaye A, Ndey Bigue MAR, et al. (2025) Morphology of the middle cerebral artery (sylvian artery) on MRI: interest in surgery and imaging. Anat Physiol Open Access J 2(1): 1-7.
15. Kaplan HA (1965) The lateral perforating branches of the anterior and middle cerebral arteries. J Neurosurg 23(3): 305-310.
16. Tomaszewski KA, Henry BM, Ramakrishnan PK, Roy J, Vikse J, et al. (2017) Development of the Anatomical Quality Assurance (AQUA) checklist: guidelines for reporting original anatomical studies. Clin Anat 30(1) : 14-20.
17. von Elm E, Altman DG, Egger M, Pocock SJ, Gotzsche PC, et al. (2007) The Strengthening the Reporting of Observational Studies in Epidemiology (STROBE) statement : guidelines for reporting observational studies. Lancet 370(9596) : 1453-1457.
18. Wade-Kane R, Seye C, Gaye M, Ainina N, Astou GTS, et al. (2022) Morphometry of the middle cerebral artery (sylvian artery) on MRI : contribution to cerebral endovascular surgery. J Neurol Neurol Sci Disord 8(1): 001-006.
19. Rouvière H, Delmas A. Anatomie humaine. Descriptive, topographique et fonctionnelle. Système nerveux central. 15e éd. Paris : Masson ; 2002.
20. Vitte E, Chevallier JM (1998) Neuro-anatomie. 4e éd. Paris ; Flammarion.
21. Diaz-Otero JM, Garver H, Fink GD, Jackson WF, Dorrance AM (2016) Aging is associated with changes to the biomechanical properties of the posterior cerebral artery and parenchymal arterioles. Am J Physiol Heart Circ Physiol 310(3): H365-H375.